2011 American Control Conference
on O'Farrell Street, San Francisco, CA, USA
June 29 - July 01, 2011

Application of Complex-Valued FXLMS Adaptive Filter to Fourier Basis Control of Adaptive Optics

Masaki Nagashima and Brij Agrawal

Abstract— **In this paper, the Filtered-X Least Mean Square (FXLMS) adaptive filter with bias integration technique is applied to an adaptive optics system where the Discrete Fourier Transform is used to project the measured phase onto the Fourier basis for modal control. The control law is applied in the complex-valued coefficient space and the FXLMS algorithm is modified accordingly for the complex-valued control. Numerical analysis is conducted for a feedback loop of a single Fourier mode in the presence of a disturbance representing a frozen flow atmospheric turbulence. The performance is compared with a Kalman estimator based control law proposed in the literature called Predictive Fourier Control (PFC). The proposed method demonstrated a similar performance for a stationary disturbance and improved performance for a slowly drifting disturbance. Whereas the performance of the PFC is very sensitive to the accuracy of the identification of the disturbance, the proposed method does not require such an explicit identification and produces minimum error for the given disturbance.**

Index Terms— **Adaptive Optics, Adaptive Filter, Filtered-X LMS, Predictive Fourier Control.**

I. Introduction

Adaptive Optics (AO) refers to optical control systems used for advanced telescopes or laser propagation systems where the phase aberration of the optical waves is measured by wave-front sensors (WFSs) and corrected by deformable mirrors (DMs). In recent years, control techniques that are more advanced than a simple classical control have been proposed [1-10]. Due to the increased size of the arrays in WFSs and DMs, the computational cost of control schemes has become important in large AO applications, and the two-dimensional Discrete Fourier Transform has been introduced as a computationally efficient way for reconstructing the phase from the phase gradient measurement by Shack-Hartmann WFSs [11], [12].

Poyneer *et al*. pointed out another benefit of Fourier decomposition for a class of disturbance and proposed a control scheme called Predictive Fourier Control (PFC) [9]. In the Fourier coefficient space, an atmospheric turbulence that obeys the frozen flow hypothesis exhibits distinctive peaks in the temporal frequency spectrum corresponding to each turbulence layer, and the PFC takes advantage of this observation for efficient modeling of the disturbance in the Fourier coefficient space. The identified disturbance is used to construct a Kalman filter which performs one-step-ahead prediction of the disturbance state to suppress the disturbance [9], [13]. Because the Fourier Transform is spatially orthogonal, the AO system is uncoupled in the Fourier domain and computational load for the control law is significantly reduced compared with full-state Multi-Input Multi-Output (MIMO) control laws. The PFC is optimized for the current temporal dynamics of the disturbance and it requires repetition of disturbance identification and computation of the controller parameters.

The purpose of this paper is to introduce an adaptive controller for the DFT based modal AO control system referred to here as Fourier basis AO control. Because of its adaptive nature, the proposed Filtered-X Least Mean Square (FXLMS) method can eliminate the need for the explicit disturbance identification and controller update required by the PFC. The development is based on the assumptions that the controller is applied on the completely uncoupled Fourier modes and that a class of disturbance exists which exhibits distinctive peaks in the Fourier domain. While whether these assumptions are appropriate or not is an important question in practice, it is out of scope of this paper and is not addressed. Given the uncoupling assumption, a Single-Input Single-Output (SISO) loop for an arbitrary mode is used to investigate the behavior of the control law. A Fourier basis AO control system is described in the next section followed by the description of the proposed control law. A brief description of the PFC is also provided. Numerical simulation results are presented in Section IV and Section V provides a discussion of the results.

II. Fourier Basis control of Adaptive Optics

Fig. 1 shows the block diagram of a Fourier basis AO control system considered in this study.

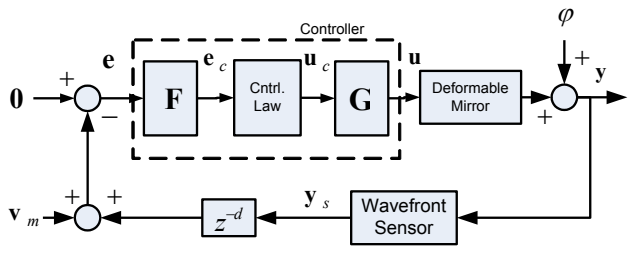

Fig. 1. Block diagram of a Fourier basis Adaptive Optics control system.

The dynamics of the DM and the WFS are all assumed to be negligible except for the pure time delay denoted by d, and the relationship from the actuator command $\mathbf{u}$ to the sensor output $\mathbf{y}_s$, which can either be phase or phase gradient, is represented by a constant influence matrix $\mathbf{M}$. The disturbance is denoted by φ, and $\mathbf{e}$ and $\mathbf{v}_m$ are the error and measurement noise, respectively. For an AO system with m sensor output signals and n actuator input signals, $\mathbf{M}$ is an $m \times n$ matrix and the sensor output and the actuator command are represented by vectors in $\Re^m$ and $\Re^n$, respectively.

Commonly, the sensor output is transformed to a different vector space by a matrix $\mathbf{F}$ whose dimension is $k \times m$ to apply a control law. The controller output is then converted to the actual command for the actuators by a matrix $\mathbf{G}$. If the rank of $\mathbf{F}$ is k and it is smaller than that of $\mathbf{M}$, the path from $\mathbf{u}$ to $\mathbf{y}_s$ which is $\mathbf{FM}$ can be diagonalized by the pseudo inverse of $\mathbf{FM}$, i.e., $\mathbf{FM}(\mathbf{FM})^\dagger = \mathbf{I}$, where † denotes the pseudo inverse and $\mathbf{I}$ is an identity matrix of dimension $k \times k$. Thus, choosing $(\mathbf{FM})^\dagger$ as $\mathbf{G}$ will uncouple the path from $\mathbf{u}_c$ to $\mathbf{e}_c$, and a SISO controller can be applied individually on each component of $\mathbf{e}_c$. For example, let $\mathbf{F} = \mathbf{M}^\dagger$, then $\mathbf{G} = (\mathbf{M}^\dagger\mathbf{M})^\dagger = \mathbf{I}$ for $\mathbf{M}$ whose rank is $n <= m$ and the open loop path is $\mathbf{FMG} = \mathbf{M}^\dagger\mathbf{M}(\mathbf{M}^\dagger\mathbf{M})^\dagger = \mathbf{I}$.

If the rank of $\mathbf{M}$ is $r < n$, then modal reduction techniques such as the singular value decomposition can be applied. For instance, suppose $\mathbf{F} = \mathbf{U}'^T$, where $\mathbf{U}'$ is the transpose of the first r column vectors of $\mathbf{U}$ which is obtained by the singular value decomposition $\mathbf{M} = \mathbf{U}\mathbf{\Sigma}\mathbf{V}^T$. Because of the orthogonality of $\mathbf{U}$ and $\mathbf{V}$, it can be shown that $\mathbf{FMG} = \mathbf{U}'^T(\mathbf{U}\mathbf{\Sigma}\mathbf{V}^T)(\mathbf{U}'^T\mathbf{U}\mathbf{\Sigma}\mathbf{V}^T)^\dagger = \mathbf{I}$. Wavefront sensors usually cannot observe piston mode whereas the DM may be able to produce it. In this case, the rank of $\mathbf{M}$ cannot exceed n-1 even for $\mathbf{M}$ with $n < m$, and the dimension of controller vector space needs to be reduced to less than the number of the actuators in the DM to achieve the uncoupling of the system.

In the Fourier basis control, $\mathbf{F}$ represents the transform of the sensor output to the Fourier coefficients of the phase. If the sensor output is the phase, the two dimensional Discrete Fourier Transform can directly be applied and $\mathbf{F}$ becomes a matrix equivalent of the transform. When the sensor output is not the phase but the gradient of the phase as is usually the case with the wavefront sensors available today, the techniques to obtain the Fourier coefficients from the gradient information presented in [12] can be used. Due to the limited space, the details are omitted but interested readers are referred to the literature. Also, practical issues such as spillover effect of the DM or spatial aliasing of the aberration are not considered here. A detailed discussion on the latter can be found in [14]. In general, choosing a DM that has a geometry and specifications suitable for this particular control method is important for successful application. In the following, it is assumed the above mentioned techniques are applied and the uncoupling of the open loop path is achieved to the sufficient extent.

One of the benefits of applying a controller in the Fourier coefficient space is that a class of disturbance exhibits distinctive temporal frequency peaks which can be represented by a low order model with sufficiently high accuracy [9]. This result, however, is obtained for square-grid measurement points whereas hexagonal array geometry is often found in AO systems. Thus, it is of interest to investigate if the temporal characteristics of the frozen flow disturbance in the Fourier coefficient space shown in [9] are preserved even in the case of hexagonal geometry.

Suppose a very simple cosine phase function moving with velocities v_x and v_y in x and y direction, respectively, whose spatially sampled function is given as follows.

$$\phi(m,n,t) = \frac{1}{2}\left(e^{j\left(\frac{2\pi k'}{M}m+\frac{2\pi l'}{N}n-\gamma t\right)} + e^{-j\left(\frac{2\pi k'}{M}m+\frac{2\pi l'}{N}n-\gamma t\right)} \right) \quad (1)$$
$$\gamma = 2\pi k' v_x / M d_x + 2\pi l' v_y / N d_y$$

Here, M and N are the number of sample points and d_x and d_y are their intervals in the x and y directions, respectively. For simplicity, the aperture of the hexagonal array is assumed to be rectangular. The Fourier Transform of this function has a temporal frequency $\exp[-j2\pi(k' v_x / M d_x + l' v_y / N d_y)t]$.

In a hexagonal array, the sampling points of the alternate rows are shifted in the x direction by one half of the sampling interval. Let this spatial shift be Δx and its normalized value with respect to the interval be $\Delta m = \Delta x / d_x$. Then, the DFT of the hexagonal array can be expressed as follows using the shift property of DFT.

$$\Phi_{hex}(k,l,t) = \sum_n^{N-1} c(n)\left(\sum_m^{M-1} \phi(m,n,t) e^{-j\frac{2\pi k}{M}m} \right) e^{-j\frac{2\pi l}{N}n} \quad (2)$$

$$c(n) = \frac{1}{2}\left(1 - e^{j\pi(n+1)}\right) + \frac{1}{2}\left(1 - e^{j\pi n}\right) e^{-j\frac{2\pi k}{M}\Delta m} = \begin{cases} e^{-\frac{2\pi k}{M}\Delta m} & (n = odd) \\ 1 & (n = even) \end{cases} \quad (3)$$

The function $c(n)$ alternately applies the shift in the x direction. Substituting (3) into (2) yields

$$\Phi_{hex}(k,l,t) = \frac{1}{2}\left(1 + e^{-j\frac{2\pi k}{M}\Delta m}\right)\Phi(k,l,t) - \frac{1}{2}\left(e^{j\pi} + e^{-j\frac{2\pi k}{M}\Delta m}\right)\Phi'(k,l,t). \quad (4)$$

Here, $\Phi(k,l,t)$ denotes the Fourier transform of the phase on the rectangular grid and

$$\Phi'(k,l,t) = \sum_n^{N-1}\sum_m^{M-1} e^{j\pi n}\phi(m,n,t) e^{-j\left(\frac{2\pi k}{M}m+\frac{2\pi l}{N}n\right)} \quad (5)$$

is $\Phi(k,l,t)$ shifted in the l direction in the frequency domain. It can be seen from this result that the geometry change of the

measurement points introduces extra frequency components along with the magnitude and phase changes, but the temporal frequency $\exp[-j2\pi(k'v_x/Nd_x + l'v_y/Md_y)t]$ caused by the movement of the layer with velocities v_x and v_y is preserved in Eq. (4) to be exploited for disturbance attenuation.

III. Fourier Coefficient Space Controller

When complete uncoupling of the system is achieved, the MIMO system becomes a set of complex-valued SISO systems in the Fourier coefficient space as shown in Fig. 2.

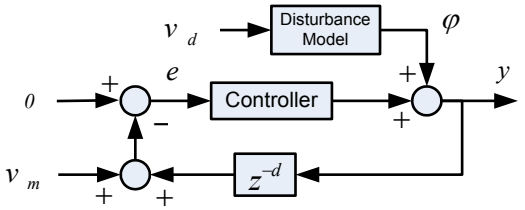

Fig. 2. Diagram of the simulation model. All variables are complex-valued and the disturbance and measurement noise represent those projected onto the Fourier basis.

Here, the projections of the disturbance and reconstructed phase onto the Fourier basis are denoted by φ and y, respectively. The v_d is the white noise driving the disturbance model and v_m is the white measurement noise. White noise is used here instead of other disturbance models in order to evaluate the ideal performance of the PFC which is based on this white noise assumption. Any delay in the actual physical system is represented by an integer d.

A. Normalized FX LMS with Bias Integration

A block diagram of the normalized FXLMS adaptive filter proposed in this paper, which augments an existing integral control feedback loop, is shown in Fig. 3. The actuator and sensor delays are represented by pure time delay d_1 and d_2.

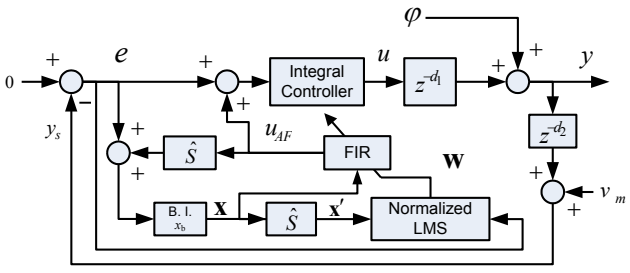

Fig. 3. Block diagram of normalized Filtered-X LMS adaptive filter augmenting an existing integral control feedback loop. B. I. stands for bias integration.

The control law of the adaptive filter loop is a Finite Impulse Response (FIR) filter given by Eq. (6), whose input signal and adaptive coefficients $w_i(k)$ called weights are expressed as vectors defined in Eq. (7) and Eq. (8).

$$u_{AF}(k) = \sum_{i=0}^{L} w_i(k)x(k-i) + w_b(k)x_b = \mathbf{w}^T[k]\mathbf{x}[k] \tag{6}$$

The bias integration technique originally introduced by Yoon, *et al*. [15], and modified by Corley, *et al*. [5], is applied here for additional robustness, and the input and weight vectors are augmented by the bias terms,

$$\mathbf{x}[k] = \left[x(k), \quad \cdots, \quad x(k-L), \quad x_b\right]^T \tag{7}$$

$$\mathbf{w}[k] = \left[w_0(k), \quad \cdots, \quad w_L(k), \quad w_b(k)\right]^T \tag{8}$$

where x_b is an arbitrary constant and w_b (k) is the corresponding weight. The input of the FIR filter, called disturbance correlated signal, or reference signal, denoted by x is the estimate of the disturbance to be canceled, which is obtained as

$$x(z) = e(z) + \hat{S}[z]u_{AF}(z) = e(z) + \frac{H[z]z^{-(d_1+d_2)}}{1+H[z]z^{-(d_1+d_2)}}u_{AF}(z). \tag{9}$$

Here, $\hat{S}[z]$ is the transfer function from $u_{AF}(z)$ to $y_s(z)$, which represents so-called secondary path dynamics, and $H[z] = K_i z/(z-1)$ is the transfer function of the integral controller with gain K_i. The filter output u_{AF} is added to the input of the integral controller and the filter adaptively modifies the frequency spectrum of x such that the filter output u_{AF} cancels the disturbance observed in the error. The Filtered-X algorithm takes into account the effect of the secondary path dynamics from $u_{AF}(z)$ to $y_s(z)$ by filtering $\mathbf{x}[z]$ with $\hat{S}[z]$, i.e.,

$$\mathbf{x}'[z] = \hat{S}[z]\mathbf{x}[z] = \frac{H[z]z^{-(d_1+d_2)}}{1+H[z]z^{-(d_1+d_2)}}\mathbf{x}[z]. \tag{10}$$

The normalized Filtered-X algorithm further processes this signal $\mathbf{x}'[k]$ by the following normalization formula, where ε is a small constant to avoid division by zero.

$$\mathbf{x}''[k] = \frac{\mathbf{x}'[k]}{\mathbf{x}'^T[k]\mathbf{x}'[k] + \varepsilon} \tag{11}$$

The weight vector is updated by the Least Mean Square (LMS) algorithm, which is a steepest gradient descent method to minimize the instantaneous square error at time k, $J(k) = e(k)^2$ [16]. The weight update formula for a real-valued system is written using $\mathbf{x}''[k]$ as

$$\mathbf{w}[k+1] = \mathbf{w}[k] - \frac{\mu}{2}\frac{\partial J[k]}{\partial \mathbf{w}[k]} = \mathbf{w}[k] + \mu e[k]\mathbf{x}''[k] \tag{12}$$

where μ is the update gain and the normalization effect is ignored. For a complex-valued system, the instantaneous error

is evaluated by $J(k) = e(k)e^*(k)$, where * denotes the complex conjugate, and Eq. (12) is modified as follows [17].

$$\mathbf{w}[k+1] = \mathbf{w}[k] + \mu e[k]\mathbf{x}''^*[k] \tag{13}$$

B. Predictive Fourier Controller

The Predictive Fourier Control is a Linear Time Invariant (LTI) controller optimized for the identified disturbance and measurement noise in the Fourier coefficient space. In the following, only a brief description of the PFC is presented as a reference. The details of the method can be found in [9].

First, the parameters of the following complex-valued AutoRegressive (AR) disturbance model

$$P(z) = \sum_{k=0}^{L} P_k(z) = \sum_{k=0}^{L} \frac{\sigma_k^2}{\left|1 - \alpha_k z^{-1}\right|^2} \tag{14}$$

is identified from the temporal Power Spectrum Density (PSD) of the disturbance. Each $P_k(z)$ has a resonance peak at $f_k = \arg\{\alpha_k\}/2\pi T$ Hz, and this resonance frequency is determined by computing the cross-correlation of a template AR model and the disturbance PSD for all peaks whose magnitudes exceed a certain threshold. The static dc component is represented by $k = 0$, and L corresponds to the number of layers in the disturbance moving in different direction at various velocities. When two or more frequency peaks are very close, it appears as a single peak and L becomes less than the number of the layers.

Since this process only determines the phase of α_k, the magnitude of α_k which represents the damping of the mode is determined by an empirical formula $|\alpha_k| = 1 - |2f_k / f_S| / 20$ where f_s is the sampling frequency. The magnitude parameter σ_k^2 of each mode is obtained by fitting the corresponding AR model to the disturbance PSD. The measurement noise power σ_m^2 is estimated from the power of the disturbance at a very high frequency range where no disturbance component is expected to appear.

The obtained disturbance model is then converted to a state space form to construct a Kalman estimator which performs one-step-ahead prediction of the disturbance state whose conjugate is used to cancel the disturbance. A steady state optimal gain matrix for the Kalman estimator is obtained by solving an Algebraic Riccati Equation (ARE) formulated with the identified disturbance model and the measurement noise power. Because this state space system is SISO, the resulting controller can be expresses by the following transfer function.

$$C(z) = \frac{1}{1 + qz^{-1}} \sum_{k=0}^{L} \frac{p_k}{1 - \alpha_k z^{-1}} \tag{15}$$

IV. Numerical Simulation

Numerical simulation of the system shown in Fig. 3 was conducted with the delay $d_1 = d_2 = 1$ for a single feedback loop representing a control loop for an arbitrary Fourier mode. This is considered to be sufficient to demonstrate the qualitative behavior of the proposed method for the given class of disturbance. For the PFC, the controller replaces the integral controller and adaptive filter is removed. A disturbance representing a four-layer frozen flow atmospheric turbulence with a static phase aberration was generated to imitate the data shown in [9]. The parameters are shown in Table 1. The power of the disturbance noise v_d and the measurement noise v_m are 10^{-8} and 10^{-6}, respectively. The sample rate of the system is 1000Hz.

TABLE 1
PARAMETERS OF THE DISTURBANCE

Layers	0	1	2	3	4
$\lvert\alpha_k\rvert$	0.999	0.996	0.998	0.994	0.997
f_k (Hz)	0	-30	-10	15	50

A normalized FXLMS adaptive filter with bias integration was designed for this simulation and the parameters are shown in Table 2. The gain of the integral controller was determined so that the control loop is stable with sufficient margin.

TABLE 2
ADAPTIVE FILTER CONTROLLER PARAMETERS

Number of Weights	μ	ε	Integrator gain K_i	x_b
15	0.030	$1.2\ 10^{-7}$	0.09	0.001

The disturbance model and the controller parameters for the PFC were obtained as shown in Table 3. The hat ^ indicates the value is an estimate. The measurement noise estimate $\hat{\sigma}_m^2$ is 10^{-6}.

TABLE 3
PREDICTIVE FOURIER CONTROLLER PARAMETERS

Layers	0	1	2	3	4
$\lvert\hat{\alpha}_k\rvert$	0.999	0.997	0.999	0.9985	0.9950
$\hat{f}_k$ (Hz)	0	-30	-10	15	50
$\hat{\sigma}_k^2$ (10^{-8})	0.379	0.172	0.100	0.044	2.801
p_k	0.0516 +0.0062i	0.0830 +0.1119i	0.0225 +0.0128i	0.0157 +0.0043i	0.0327 -0.0004i
q = 0.2557 - 0.0387i					

Fig. 4 shows the disturbance PSD and the identified AR model with the estimated measurement noise. Unlike the frequency spectrum of a real-valued signal, the frequency

spectrum of a complex-valued signal is not symmetric with respect to the imaginary axis and both positive and negative frequencies are shown in the plot.

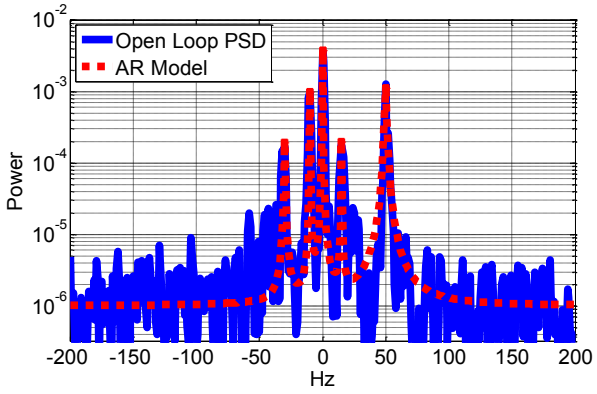

Fig. 4. AR model of the open loop disturbance PSD (dot line) and the actual disturbance PSD (solid line).

Fig. 5 shows the frequency responses of the PFC transfer functions. The PFC controller obtained using the nominal disturbance parameters in Table 1 is also shown for comparison. The sensitivity function has a slight increase around 70 Hz compared with that of the nominal PFC, which is caused by the identification error of the pole magnitudes.

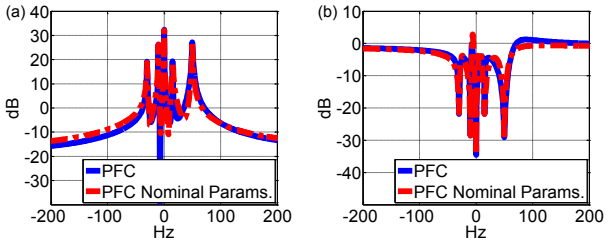

Fig. 5. PFC Frequency response. (a) PFC controller, (b) PFC feedback loop sensitivity function.

The duration of the simulation was 15 seconds. The integral controller of the proposed method was turned on at 2.0 s and the adaptive filter was turned on at 2.1 s. For the PFC, the controller was turned on at 2.0 s. Fig. 6 shows the frequency spectra and the transient responses of the output y by the proposed method and the PFC. The steady state mean square error is computed from the output between 14 s and 15 s. The proposed method produces a transient about 27 times larger than that of the PFC due to the high gain of the integral controller, but it converges about 9 times faster and the steady state mean square error is 35 % lower than that of the PFC. The steady state error of the PFC is higher due to the increase of the frequency component around 70 Hz as shown in (a) of Fig. 6, which is caused by the bump of the sensitivity function shown in (b) of Fig. 5.

Fig. 7 shows the result by the PFC with the nominal disturbance parameters. The error increase around 70 Hz is now disappeared and the controller achieves a steady state error lower than that of the proposed method in Fig. 6. The proposed method, however, also reduced the error when the number of weights was increased to 30. The steady state mean square errors of both methods approach the measurement noise level $\sigma_m^2 = 10^{-6}$.

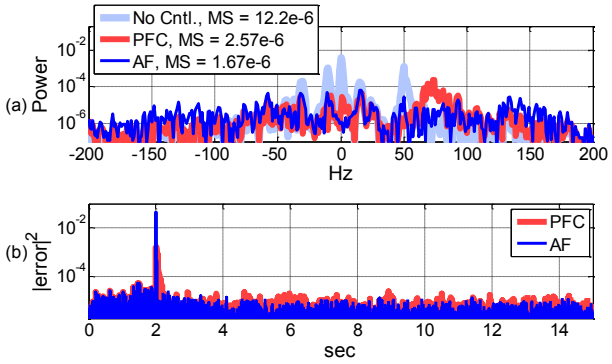

Fig. 6. Disturbance attenuation by PFC (identified disturbance parameters) and proposed method (15 weights): (a) Power Spectral Density of the output, (b) Transients of the squared output.

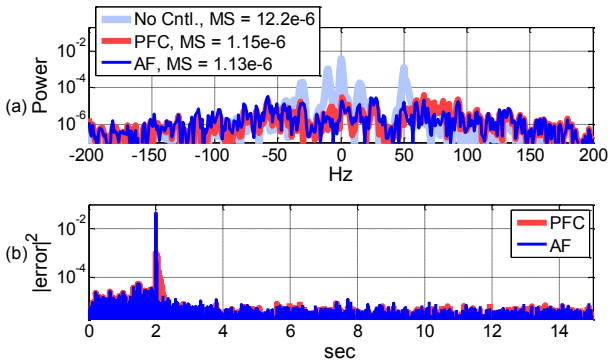

Fig. 7. Disturbance attenuation by PFC (nominal disturbance parameters) and proposed method (30 weights): (a) Power Spectral Density of the output, (b) Transients of the squared output.

Fig. 8 shows the effect of the number of weights on the steady state mean square error of the proposed controller. The error decreases as the number of weights increases until it reaches the lower limit at about 30 weights.

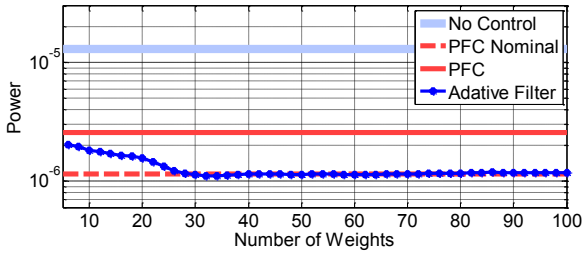

Fig. 8. Effect of the number of weights on steady state error.

The results so far addressed a disturbance with a stationary frequency spectrum. The performances of the proposed method with 30 weights and the PFC with the nominal disturbance parameters were investigated for a disturbance with drifting frequency peaks. The rate of change introduced was 0.3 Hz/s in randomly selected positive or negative

directions for all frequencies except the dc component whose frequency did not change.

Fig. 9 shows the frequency spectra and transients of the output *y*. The frequencies start drifting at 5 s and continue through 15 s. As expected, the error by the PFC increases with time after 5 s, whereas the proposed method maintains the same error level. The error level, however, is slightly increased. This is due to the fact that when the disturbance frequencies start drifting, the weights never completely converge, which results in a residual error. This error increases as the rate of the frequency change increases.

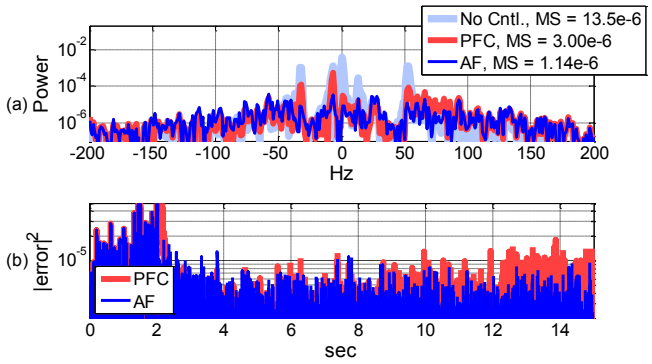

Fig. 9. Disturbance attenuation by PFC (nominal disturbance parameters) and proposed method (30 weights) for drifting disturbance: (a) Power Spectral Density of the output, (b) Transients of the squared output.

V. Conclusion

A normalized FXLMS adaptive filter with bias integration was proposed for a Fourier basis AO control system under a multi-layer frozen flow atmospheric disturbance. The performance of the proposed control law was investigated through a numerical simulation of a single Fourier coefficient control loop representing an ideal decomposition of the phase by the Fourier Transform and compared with the performance of the Predictive Fourier Control proposed in [9].

For a stationary disturbance, the maximum attenuation that can be achieved by the proposed method and the PFC is almost the same regardless of the differences that the former is an FIR filter whose coefficients are adaptively updated and the latter is an Infinite Impulse Response (IIR) filter whose coefficients are time-invariant and determined by solving the optimal estimator problem formulated with the identified disturbance model.

Compared with the PFC, the procedure for the proposed method to determine the number of weights and the update gain is not well established. Applying very conservative values may result in unnecessary computation due to extra weights and/or a very slow convergence caused by a too small gain. Some initial tuning is thus necessary. The parameters to be tuned, however, are only two scalars and the required effort is minimal. The PFC, on the other hand, is sensitive to the accuracy of the identified disturbance model. When the identification error is too large, direct tuning of the controller to improve the performance is not as simple as the tuning of the proposed method.

An important advantage of the proposed method is that it can follow a disturbance with drifting frequencies. The error increases, but does not grow with time. The error by the PFC, on the other hand, increases with time for a drifting disturbance until the disturbance identification is conducted again to re-calculate the controller parameters, which increases the computational cost.

References

[1] J. S. Gibson, C.-C. Chang, and B. L. Ellerbroek, "Adaptive optics: wave-front correction by use of adaptive filtering and control," *Applied optics*, vol. 39, no. 16, pp. 2525-38, Jun. 2000.

[2] J. S. Gibson, C.-C. Chang, and N. Chen, "Adaptive optics with a new modal decomposition of actuator and sensor spaces," in *Proceedings of the 2001 American Control Conference*, 2001, pp. 4619-4625.

[3] Y.-T. Liu and J. S. Gibson, "Adaptive control in adaptive optics for directed-energy systems," *Optical Engineering*, vol. 46, no. 4, p. 046601, 2007.

[4] B. Agrawal and T. Martinez, "Optical Beam Control Testbeds," in *AIAA Guidance, Navigation, and Control Conference, Aug. 18-21, Honolulu, Hawaii*, Honolulu, Hawaii, USA, 2008.

[5] C. M. S. Corley, M. Nagashima, and B. N. Agrawal, "Beam control and a new laboratory testbed for adaptive optics in a maritime environment," presented at the 2010 IEEE Aerospace Conference, Big Sky, Montana, USA, 2010.

[6] D. P. Looze and N. Merritt, "Gain optimization for adaptive optics systems," in *American Control Conference, 2003. Proceedings of the 2003*, 2003, vol. 4, pp. 3370-3374 vol.4.

[7] B. Le Roux, J.-M. Conan, C. Kulcsár, H.-F. Raynaud, L. M. Mugnier, and T. Fusco, "Optimal control law for classical and multiconjugate adaptive optics.," *Journal of the Optical Society of America. A, Optics, image science, and vision*, vol. 21, no. 7, pp. 1261-76, Jul. 2004.

[8] L. A. Poyneer and J.-P. Véran, "Optimal modal fourier-transform wavefront control," *Journal of the Optical Society of America. A, Optics, image science, and vision*, vol. 22, no. 8, pp. 1515-26, 2005.

[9] L. A. Poyneer, B. A. Macintosh, and J.-P. Véran, "Fourier transform wavefront control with adaptive prediction of the atmosphere," *Journal of the Optical Society of America. A, Optics, image science, and vision*, vol. 24, no. 9, pp. 2645-60, 2007.

[10] N. Doelman, R. Fraanje, I. Houtzager, and M. Verhaegen, "Adaptive and Real-time Optimal Control for Adaptive Optics Systems," *European Journal of Control*, vol. 15, no. 3-4, pp. 480-488, 2009.

[11] K. R. Freischlad, "Wave-front integration from difference data," in *Interferometry: Techniques and Analysis*, San Diego, CA, USA, 1993, vol. 1755, pp. 212-218.

[12] L. A. Poyneer, D. T. Gavel, and J. M. Brase, "Fast wave-front reconstruction in large adaptive optics systems with use of the Fourier transform," *October*, vol. 19, no. 10, pp. 2100-2111, 2002.

[13] L. Poyneer and J.-P. Véran, "Predictive wavefront control for adaptive optics with arbitrary control loop delays," *Journal of the Optical Society of America. A, Optics, image science, and vision*, vol. 25, no. 7, pp. 1486-96, Jul. 2008.

[14] L. Poyneer and B. Macintosh, "Spatially filtered wave-front sensor for high-order adaptive optics," *Journal of the Optical Society of America. A, Optics, image science, and vision*, vol. 21, no. 5, pp. 810-819, 2004.

[15] H. Yoon, B. E. Bateman, and B. N. Agrawal, "Laser Beam Jitter Control Using Recursive-Least-Square Adaptive Filters," in *2008 Directed Energy Systems Symposium Beam Control Conference Proceedings*, Monterey, California, CA, 2008.

[16] S. M. Kuo and D. R. Morgan, *Active Noise Control Systems: Algorithms and DSP Implementations*. Wiley-Interscience, 1996.

[17] B. Widrow, J. McCool, and M. Ball, "The complex LMS algorithm," *Proceedings of the IEEE*, vol. 63, no. 4, pp. 719-720, 1975.